COINCIDING TRANSPORTS OF WATER VAPOR AND AEROSOLS TO THE ARCTIC

– in observations, reanalysis data and earth system model simulations

Scientific Report from DCE – Danish Centre for Environment and Energy No. 638 2025

AARHUS
UNIVERSITY
DCE – DANISH CENTRE FOR ENVIRONMENT AND ENERGY

Scientific Report from DCE – Danish Centre for Environment and Energy No. 638, 2025

Coinciding transports of water vapor and aerosols to the Arctic

- in observations, reanalysis data and earth system model simulations

Peter L. Langen
Thea Quistgaard
Ulas Im

Aarhus University, Department of Environmental Science

Data sheet

Series title and no.:	Scientific Report from DCE – Danish Centre for Environment and Energy No. 638
Category:	Research contribution
Title:	Coinciding transports of water vapor and aerosols to the Arctic
Subtitle:	- in observations, reanalysis data and earth system model simulations
Authors:	Peter L. Langen, Thea Quistgaard og Ulas Im
Institution:	Aarhus University, Department of Environmental Science
Publisher:	Aarhus University, DCE – Danish Centre for Environment and Energy ©
URL:	http://dce.au.dk/en
Year of publication:	January 2025
Editing completed:	January 2025
Referee:	Kaj Mantzius Hansen
Quality assurance, DCE:	Kirsten Bang
Financial support:	Klimastøtte til Arktis (Climate support for the Arctic), Danish Energy Agency)
Please cite as:	Langen, P.L., Quistgaard, T. & Im. U.. 2025. Coinciding transports of water vapor and aerosols to the Arctic - in observations, reanalysis data and earth system model simulations. Aarhus University, DCE – Danish Centre for Environment and Energy, 31 pp. Scientific Report No. 638

Abstract: This study investigates statistics of moisture and aerosol transports to the Arctic. In an atmospheric reanalysis product, we find a significant positive relationship, with increased column-total aerosol amounts during high northward water vapor transport events, for most of the species considered. In an Earth System Model, we find that the positive relationship between aerosols and high northward water vapor transport from the reanalysis is rather a significantly negative relationship and, further, that increasing the aerosol amounts appears not to influence how large that increase in cloudiness is during high water vapor transport events. However, there are still many unanswered questions and much work to do to fully understand the discrepancy between the model and the reanalysis, and several processes related to aerosol-cloud interactions are still under development.

Keywords:	Atmospheric northward water transport events, Long-range aerosol transports to the Arctic, Aerosol-cloud-climate interactions, Atmospheric reanalysis, Earth System Models
Layout:	Ann-Katrine Holme Christoffersen, Aarhus University, Department of Environmental Science
Front page photo:	Ann-Katrine Holme Christoffersen, Aarhus University, Department of Environmental Science
ISBN:	978-87-7156-920-9
ISSN (electronic):	2244-9981
Number of pages:	31

Contents

Sammenfatning

Der mangler stadig en videnskabelig konsensus om forbindelsen mellem arktisk klima og vejret på mellembreddegrader. Ikke desto mindre synes vanddampflux fra mellembreddegrader under episodiske begivenheder at spille en vigtig rolle for det arktiske klima, ligesom aerosoler, der delvist transporteres til Arktis fra lavere breddegrader, gør. Men selvom vanddamp og aerosoler kan transporteres til Arktis under de samme vejrforhold, er den kombinerede effekt af de to endnu ikke blevet undersøgt.

Denne undersøgelse analyserer statistikken for samtidig transport af vanddamp og aerosoler til den europæisk-atlantiske sektor af Arktis ved hjælp af station-baserede observationer af aerosoler, reanalyser og simuleringer med en jord-system-model.

Vi finder, at observationsperiodens længde er for kort til at drage robuste konklusioner herudfra. I reanalyse-baserede aerosoler finder vi en signifikant positiv sammenhæng med øgede aerosolmængder under begivenheder med høj nordgående vanddamptransport for de fleste af de betragtede aerosoler.

I jord-system-modellen finder vi ikke blot, at de statistiske karakteristika for aersoltidsserierne adskiller sig fra reanalysen, men også at den positive sammenhæng mellem aerosoler og høj nordgående vanddamptransport fra reanalysen snarere viser sig som en signifikant negativ sammenhæng. Under høj-transportbegivenheder viser modellen, ikke overraskende, øget skydække, men en stigning i mængden af aerosoler synes ikke at påvirke, hvor meget skydækket øges.

Hvis det sidstnævnte generelt er sandt, ville det betyde, at selvom reanalysen antyder øgede mængder aerosoler under høj vanddamptransport, vil dette ikke føre til øget skydække og derfor ikke påvirke det arktiske klima ad den vej. Dog er der stadig mange ubesvarede spørgsmål og meget arbejde at gøre for fuldt ud at forstå uoverensstemmelserne mellem modellen og reanalysen, og flere processer relateret til aerosol-sky-interaktioner er stadig under udvikling. Derfor er ovenstående konklusion sandsynligvis ikke det sidste ord i denne sag.

Summary

The connection between Arctic climate and mid-latitude weather continues to be an issue of concern as scientific consensus on the matter is still lacking. Nevertheless, fluxes of moisture coming from mid-latitudes during episodic events do appear to play an important role for Arctic climate as do aerosols partly transported into the Arctic from lower latitudes. However, while moisture and aerosols may enter into the Arctic under the same weather conditions, the combined effect of the two has currently not been studied.

This study investigates the statistics of moisture and aerosol co-transports to the European-Atlantic sector of the Arctic in station-based observed aerosols, reanalyses and Earth System Model simulations.

We find that the length of the observational record is too short to make robust claims based thereon. In the reanalysis-based aerosols we find a significant positive relationship, with increased column-total aerosol amounts during high northward water vapor transport events, for most of the species considered.

In the Earth System Model, we find that not only are the characteristics of the time series different from the reanalysis, the positive relationship between aerosols and high northward water vapor transport from the reanalysis is rather a significantly negative relationship. During high transport events, the model unsurprisingly displays increased cloudiness, but increasing the aerosol amounts appears not to influence how large that increase in cloudiness is.

If the latter is generally true, this would mean that, even if, as the reanalysis may suggest, there is increased aerosol amount during high water vapor transport, this would not lead to increased cloudiness and would not by that pathway impact Arctic climate. However, there are still many unanswered questions and much work to do to fully understand the discrepancy between the model and the reanalysis, and several processes related to aerosol-cloud interactions are still under development. Therefore, the above conclusion is unlikely to be the final word on the matter.

1 Introduction

The Arctic is warming three to four times faster than the global average (AMAP 2017; Lenssen et al. 2019; Rantanen et al. 2022) with implications for both environment and society. The warming not only affects the Arctic, intensifying ice melt and contributing to global sea level rise (AMAP 2021), it has also been linked to extreme weather events in Europe, North America and Asia (e.g., Francis and Vavrus 2012). Water vapor carried by winds is the main way temperate zones influence Arctic warming (e.g., Langen and Alexeev 2007; Graversen and Burtu 2016; Yoshimori et al. 2017; Taylor et al. 2022) and water vapor coming from mid-latitudes during week-long moisture intrusion events has been shown to impact Arctic temperatures and sea ice cover (Woods and Caballero 2016; Graversen and Burtu 2016; Baggett and Lee 2017).

Aerosols affect climate by scattering incoming solar radiation, as well as changing the cloud properties and thus indirectly affecting the scattering of radiation. After being deposited on snow and ice surfaces, black carbon (BC) can amplify ice melt by lowering the albedo and increasing solar heating of the surface, which is an important factor over the Arctic. Aerosols also affect cloud properties, including their droplet size, lifetime, and vertical extent, thereby influencing both the shortwave cooling and longwave warming effects of clouds. Moreover, Arctic cloud impacts are distinct from global impacts, owing to the extreme seasonality of solar radiation in the Arctic, unique characteristics of Arctic clouds (e.g., high frequency of mixed-phase occurrence), and rapidly evolving sea-ice distributions. Together, they lead to complicated and unique phenomena that govern Arctic aerosol abundances and climate impacts. The changes taking place in the Arctic have consequences for how aerosols affect the region. For example, reductions in sea-ice extent, thawing of permafrost, and humidification of the Arctic troposphere can affect the emissions, lifetime and radiative forcing of aerosols within the Arctic.

Aerosols are emitted from both anthropogenic (man-made) and natural sources, although in differing proportions. Some aerosol species, such as BC, or their precursors such as sulfur dioxide (SO_2), are emitted mostly from the combustion of fossil fuels and biofuels in energy production, industry, residential heating, and traffic. However, substantial emissions of BC and organic carbon (OC) come from naturally occurring or man-made forest fires, or volcanic eruptions. Another globally large aerosol source is mineral dust, which derives both from naturally occurring desert soils and those made erodible by human activity and agriculture, as well as sea-salt, which is emitted from the oceans. Another natural source of secondary aerosols is precursor gases from biogenic activities from vegetation and marine sources.

Over the Arctic, the anthropogenic aerosols, as well as mineral dust, are long-range transported from mid-latitudes during the spring period, when the Arctic dome expands due to decreasing temperature difference, to cover the mid-latitude emission sources and allows their transportation into the Arctic. This period is called the Arctic Haze period. In summer, however, Arctic aerosols are mainly driven by local sources, particularly marine sources of sea-salt and organic precursors of secondary organic aerosols, as atmospheric transport patterns change, and precipitation is more frequent, removing the aerosols from the atmosphere while transported.

While no scientific consensus exists on the link between Arctic and mid-latitude weather (AMAP 2021), studies show that both moisture coming from mid-latitudes during week-long moisture intrusion events (Woods and Caballero 2016) and aerosols partly transported from lower latitudes (Im et al. 2021; Lapere et al. 2024) impact the Arctic. During moisture events, the Arctic is warmer and moister, and clouds are both geometrically and optically thicker than in background conditions (Dekoutsidis et al. 2024). While moisture and aerosols may enter into the Arctic under the same weather conditions, the combined effect of the two has currently not been studied.

There is thus an apparent need to study co-transports of water vapor and aerosols. To that end, we investigate the statistical relationships between events of increased water vapor fluxes in observations, in reanalyses and in an Earth System Model. The observations provide us with near-surface aerosol levels at two stations in Northeast Greenland and on Svalbard. Water vapor fluxes throughout the atmosphere are not directly observed and the best estimates come from reanalysis data. We include also aerosols from a reanalysis, providing full-column, spatially and temporally gap-free estimates, since the observational aerosol record is relatively short, has some irregularities and only gives a near-surface view. Finally, we turn to an Earth System Model, since one can design experiments that allow for targeted investigations of water vapor fluxes, aerosols and clouds.

We ask the following questions:

- In observations
  - To what extent do events of increased northward water vapor fluxes (NWVF) in the European-Atlantic sector of the Arctic coincide with increased values in the observed near surface aerosols at two stations in the area?
- In a reanalysis
  - To what extent does increased NWVF coincide with increased aerosols in the European-Atlantic sector of the Arctic in a reanalysis dataset?
- In an Earth System Model
  - To what extent do the statistics of NWVF and aerosol events match those in the reanalysis?
  - Does high NWVF coincide with higher amounts of clouds?
  - Do higher aerosol levels during high NWVF events lead to further increases in cloudiness?

2 Data

2.1 Datasets

2.1.1 Observational data

We have used surface observations of elemental carbon (EC) and sulfate (SO_4) from two Arctic stations; Villum research station (VRS: 81 N, 16 W; https://villumresearchstation.dk/) in Northeast Greenland, and Zeppelin (79 N, 12 E; https://www.aces.su.se/zeppelin/index.html) in Svalbard (marked with crosses in Figure 1). While VRS is surrounded by sea-ice year-round, Zeppelin station is surrounded by open ocean. EC data at VRS and Zeppelin span the periods 2008-2022 and 2017-2022, respectively, while SO_4 data span 2000-2022 and 1993-2022, respectively. Observations are conducted at weekly resolution at VRS and daily at Zeppelin.

The Zeppelin station is located 474 m above sea level while VRS is 24 m above sea level. This means that Zeppelin may be more representative of transports outside the very bottom of the atmospheric boundary layer.

2.1.2 Reanalysis data

Weather reanalysis is a method of reconstructing past atmospheric states by assimilating historical observations into a modern numerical weather prediction (NWP) model. Observations (from sources such as weather stations, ships, satellites, and radiosondes) are combined with the laws of physics in the NWP model to produce a spatially and temporally consistent dataset. This process accounts for observational gaps and inconsistencies, providing a gridded representation of the atmosphere, land, and oceans over time. ERA5 (C3S 2017) is a state-of-the-art global reanalysis dataset produced by the European Centre for Medium-Range Weather Forecasts (ECMWF). It offers data from 1950 to the present, with updates provided in near real-time. ERA5 has a spatial resolution of approximately 31 km (0.25° x 0.25°) and provides hourly temporal resolution. Here, we use the output of the vertically integrated northward water vapor flux. This gives, in each point, the northward component of column-total transport of water vapor.

Another reanalysis, MERRA-2, includes an aerosol reanalysis using the Goddard Earth Observing System version 5 (GEOS-5) with the Goddard Aerosol Assimilation System (GAAS). Using the interactive Goddard Chemistry, Aerosol, Radiation, and Transport (GOCART) aerosol module, the GAAS includes 15 aerosol tracers (dust, sea-salt, sulfate, black and organic carbon) whose lifetime is driven by prescribed sea-surface temperature and sea-ice, daily volcanic and biomass burning emissions, as well as high-resolution inventories of anthropogenic emission sources. The GAAS includes assimilation of bias-correct aerosol optical depth (AOD) from several ground- and satellite-based sensors, including AVHRR, MODIS Aqua and Terra, MISR over bright surfaces, and AERONET. The MERRA-2 aerosol reanalysis produced by the Global Modeling and Assimilation Office (GMAO) thus provides observationally-constrained aerosol optical depth from 1980–present, with aerosol speciation determined from GOCART model.

2.1.3 Earth System Model data

We have further used the GISS-E2.1, which is the CMIP6 version of the GISS modelE Earth system model (GISS-E2.1 hereinafter), which has been validated extensively over the globe (Kelley et al. 2020) as well as over the Arctic (Im et al. 2021). GISS-E2.1 has a horizontal resolution of 2° in latitude by 2.5° in longitude and 40 layers in the vertical extending from the surface to 0.1 hPa in the lower mesosphere.

In the present work, we used the One-Moment Aerosol scheme (OMA: Bauer et al. 2020 and references therein), which is a mass-based scheme in which aerosols are assumed to remain externally mixed. The scheme treats sulfate, nitrate, ammonium, carbonaceous aerosols (black carbon and organic carbon, including the NOx-dependent formation of secondary organic aerosol (SOA) and methanesulfonic acid formation), dust and sea-salt. OMA only includes the first indirect effect, in which the aerosol number concentration that impacts clouds is obtained from the aerosol mass as described in Menon and Rotstayn (2006). The parameterization described by Menon and Rotstayn (2006) that we use only affects the cloud droplet number concentration (CDNC), not cloud droplet size, which is not explicitly calculated in GISS-E2.1. Following the change in CDNC, we do not stop the model from changing either liquid water path (LWP) or precipitation rates, since the cloud code sees the different CDNC and responds accordingly. The second indirect effect (auto conversion) is not included.

In OMA, the natural emissions of sea salt, dimethylsulfide (DMS), isoprene and dust are calculated interactively. Anthropogenic dust sources are not represented in GISS-E2.1. Dust emissions vary spatially and temporally only with the evolution of climate variables like wind speed and soil moisture (Miller et al. 2006). Dust concentrations are tuned to match the observed dust aerosol optical depth (AOD).

In addition to OMA, we have also conducted a non-interactive tracers (NINT: Kelley et al. 2020) simulation from 1995 to 2014, with noninteractive (though monthly varying) fields of radiatively active components (ozone and multiple aerosol species) read in from previously calculated runs with the OMA version of the model using the Atmospheric Model Intercomparison Project (AMIP) configuration in Bauer et al. (2020) as described in Kelley et al. (2020). The NINT model includes a tuned aerosol first indirect effect following Hansen et al. (2005).

In this study, we have performed AMIP-type simulations, which use prescribed sea surface temperature (SST) and sea ice fraction during the recent past (Rayner et al. 2003). The prescribed SST dataset in GISS-E2.1 is a merged product based on the HadISST and NOAA Optimum Interpolation (OI) Sea Surface Temperature (SST) V2 (Reynolds et al. 2002). In addition, we have performed the simulations in sub-daily diagnostics mode in order to produce daily mean aerosol, cloud, and water vapor fluxes.

2.2 Derived timeseries

To compare variability in the ERA5 reanalysis northward water vapor flux (NWVF) to that in the observed aerosols, we calculated the total NWVF across the 70N latitude in the section 45W-45E (shown by the solid red line in Figure 1). This was done by choosing the ERA5 gridcells nearest to 70N. The NWVF values here have units of kg m^{-1} s^{-1}, i.e., northward flux measured in kg per

second per meter along the latitude circle. Multiplying each value with the east-west length of the gridcell in the east-west direction and finally adding all these between 45W and 45E gives the total NWVF across the latitude section measured in kg s^{-1}.

As seen in Figure 1, the stations are located somewhat further north of the 70N boundary than the dashed analysis box. We placed the box further south in order to be able to make as clear an identification of the causation as possible. This also means that less clear signals are to be expected from the analysis of the observational series just from this effect alone.

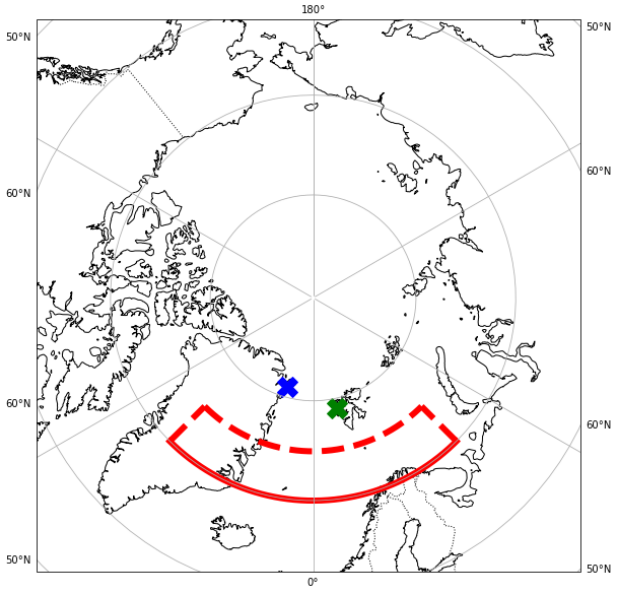

Figure 1 Illustration of the domain. The solid red line shows the line across which northward water vapor flux is integrated to produce the NWVF timeseries used throughout. The dashed red line shows the latitude-longitude box in which variables are averaged when analyzing reanalysis and model-derived aerosols and clouds. Crosses show the positions of the Villum Research Station (blue) and Zeppelin Station (green) observation sites.

The observational aerosol time series is somewhat irregular and reflects approximately weekly readings of total aerosol collection since the last reading (red curves in Figure 2). To provide the most direct comparison with these observations, the ERA5 NWVF was therefore summed over the exact dates spanned by the observational readings. This results in different NWVF timeseries corresponding to the four observed series (EC Villum, EC Zeppelin, SO_4 Villum, SO_4 Zeppelin; black curves in Figure 2).

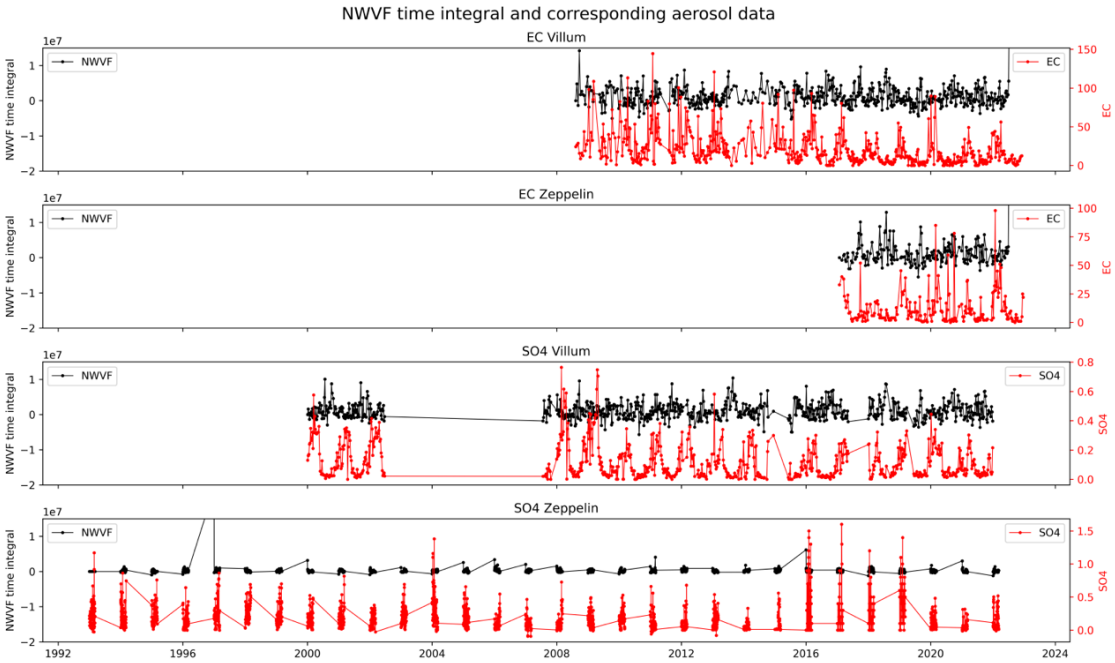

Figure 2 Black lines show NWVF filtered to match corresponding aerosol measurements, so NWVF data only contains data points if data points exist in the aerosol data and summed over the same dates as covered by the aerosol data. Red lines show the raw aerosol measurements.

Based on the resulting time series shown in Figure 2, we calculated monthly climatologies of aerosols and the respective corresponding ERA5 NWVF series. This is shown in Figure 3 for each the four aerosol timeseries, where it is clear that the temporal coverage of SO_4 Zeppelin does not allow for a proper climatology and will be excluded in the following.

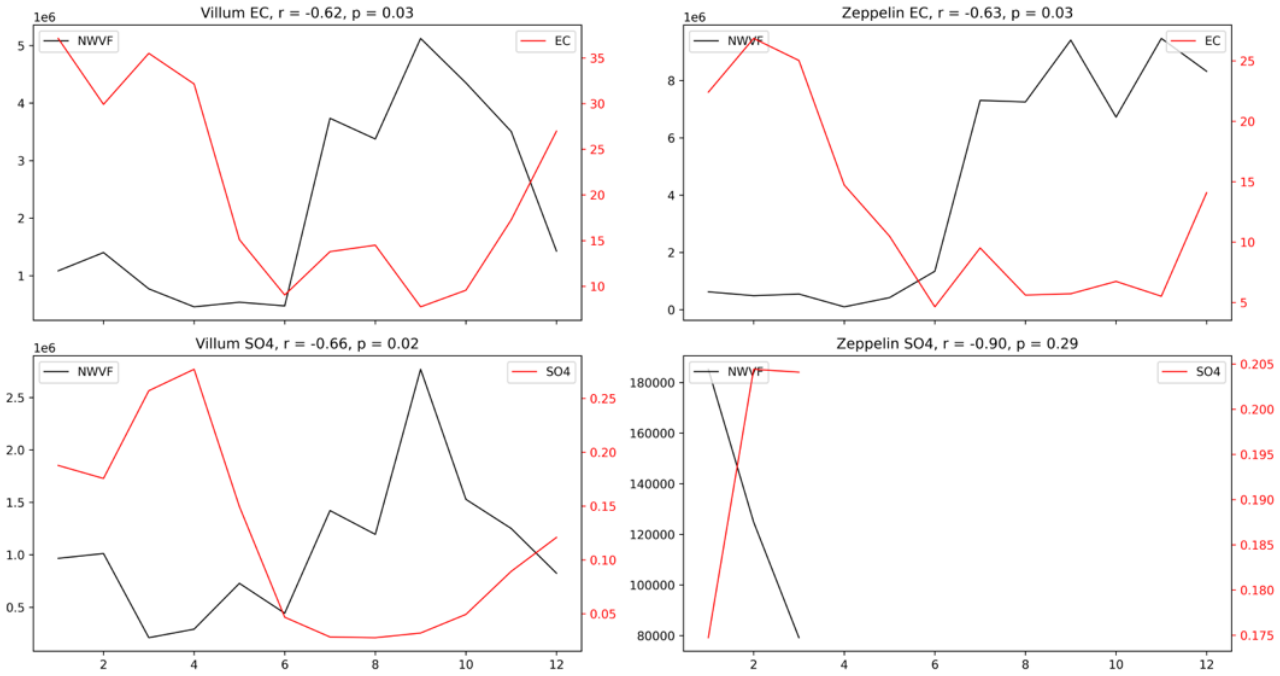

Figure 3 Monthly climatologies of NWVF and aerosol signals for the two measuring stations. Climatology is computed from the filtered NWVF data series, i.e., taking only NWVF data where aerosol data exists.

3 Analyses and results

3.1 ERA5 NWVF vs observed aerosols

The climatologies shown in Figure 3 suggest two distinct seasons with aerosol loading and NWVF displaying opposite behaviors. Aerosol loading is generally high and NWVF low in Dec-Apr, while it is generally low and NWVF high in Jul-Oct. This is the average climatology on top of which we wish to study event-wise increases in the fluxes, and what we mean by high and low fluxes must be defined against the backdrop of this climatology: During the drier winter, when NWVF generally is low, an episodic increase up to a level, which is only average for a summer situation, is likely to be a significant event – and likewise for the aerosol loadings. We therefore define two seasons as:

- Season 1: December-April
- Season 2: Juli-October

May, June and November are omitted from further analysis, as they are 'transition'-months, between high and low water vapor transport.

In the following, data from these two seasons is pooled in separate data pools and analyzed separately to estimate whether high events in water vapor transport result in significantly higher aerosol measurements. To that end, we proceed by calculating Season 1 and 2 respective means and standard deviations (std) for each series. This is shown in the left-hand panels of Figure 4, where the dotted lines illustrate the mean +/- 1 std. We use these dotted lines as thresholds to delimit "high" and "low" events in the following. However, this figure is only for illustrative purposes and shows the full series (all months) and the corresponding mean and std. In the analysis, separate means and std are used for the two seasons.

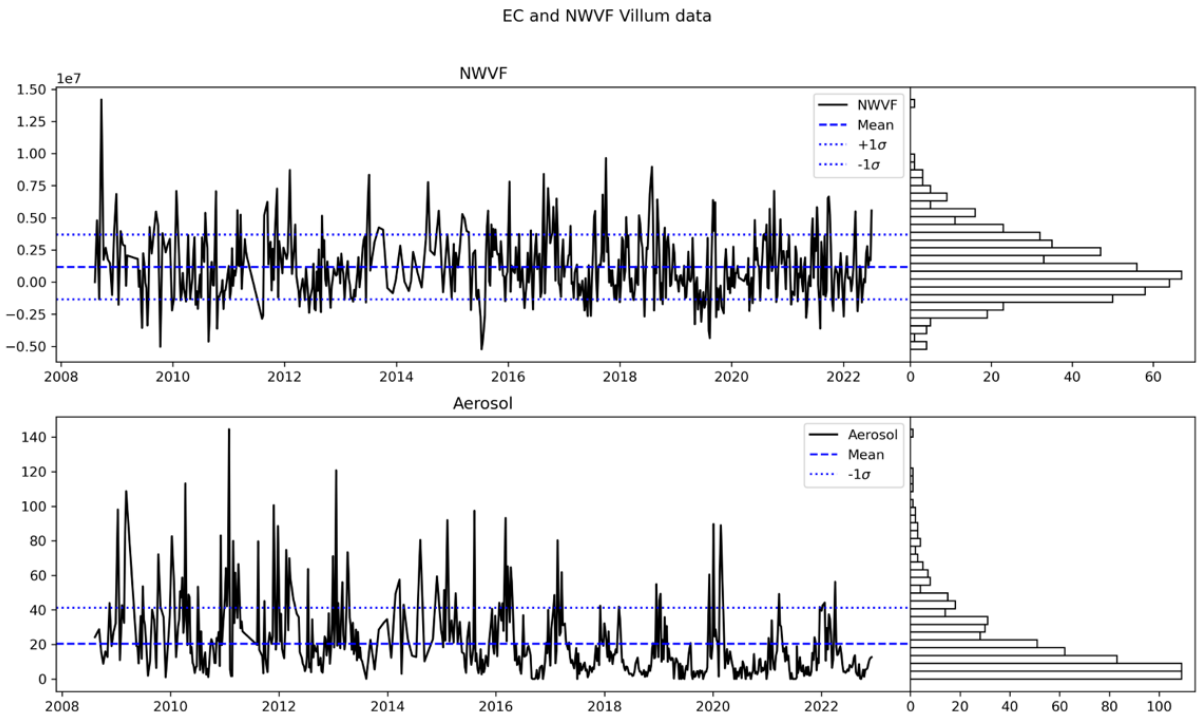

Figure 4 (Left) Full aerosol, Elemental Carbon (lower), and filtered NWVF (upper) time series from Villum station. (Right): Distribution of all data over time.

We wish to investigate whether events of high NWVF are associated with high aerosol loadings at the observation sites in the two seasons. We use the mean+1 std line to identify events of high NWVF and the histogram of events with NWVF above this threshold are shown as green bars in the upper panel in Figure 5 (for Season 1). In the lower panel of Figure 5, we show the histograms of the aerosol loadings during the high (green bars) NWVF events. If, by this analysis, high NWVF events were associated with high aerosol loadings, the green bars in the lower panel should be located in the high end. There is no indication of such a separation, and, for Season 1 EC Villum, this analysis does not indicate any tendency for increased or decreased aerosols during high NWVF events.

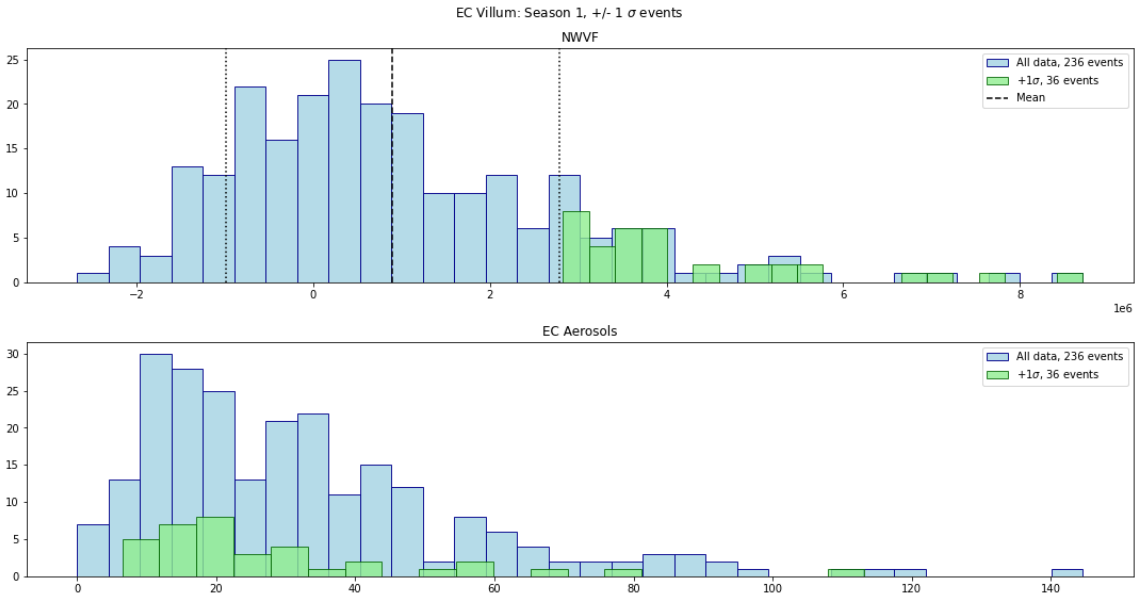

Figure 5 Histogram of NWVF and EC Villum in Season 1. (Upper): All NWVF "events" (blue), and +1 sigma events (green). (Lower): Aerosol (EC Villum) events. Blue shows all events, while green are the aerosol loadings corresponding to the dates/events that relate to the +1 sigma NWVF events (shown by green in the upper panel).

To compare two distributions (such as the blue and green histograms in the lower panel of Figure 5), one can employ the Kolmogorov-Smirnov (KS) test. Here, one converts the histograms into cumulative distribution functions (CDFs). This is illustrated in Figure 6 where the lower panel shows the CDFs corresponding to the blue and green histograms in the lower panel of Figure 5. Next, the KS test calculates the maximum vertical distance between the two CDFs and estimates the probability, p, that such a distance could occur by chance if the two samples were drawn from the same underlying distribution. When estimating this probability, the number of degrees of freedom is taken into account, and a large KS distance (vertical distance) is more likely to occur between two small samples than between two large ones. Major strengths of the KS test are that the two samples do not need to be of the same size, and one does not need to make any assumptions about the distribution (such as, for instance, Gaussianity).

In the example of the Season 1 EC at Villum shown in Figure 6, the total number of aerosol observations is 236 (blue bars in Figure 5) while the high-NWVF observations amount to 36 (green bars in Figure 5). The KS distance is 0.15 and this is estimated to have a 46 % chance of occurring randomly between such sample sizes even if they were drawn from the same distribution. As suggested by inspection of the histograms in the lower panel of Figure 5, we

thus cannot claim with statistical significance that there is an increase of aerosols at times of high NVWF compared to the general distribution.

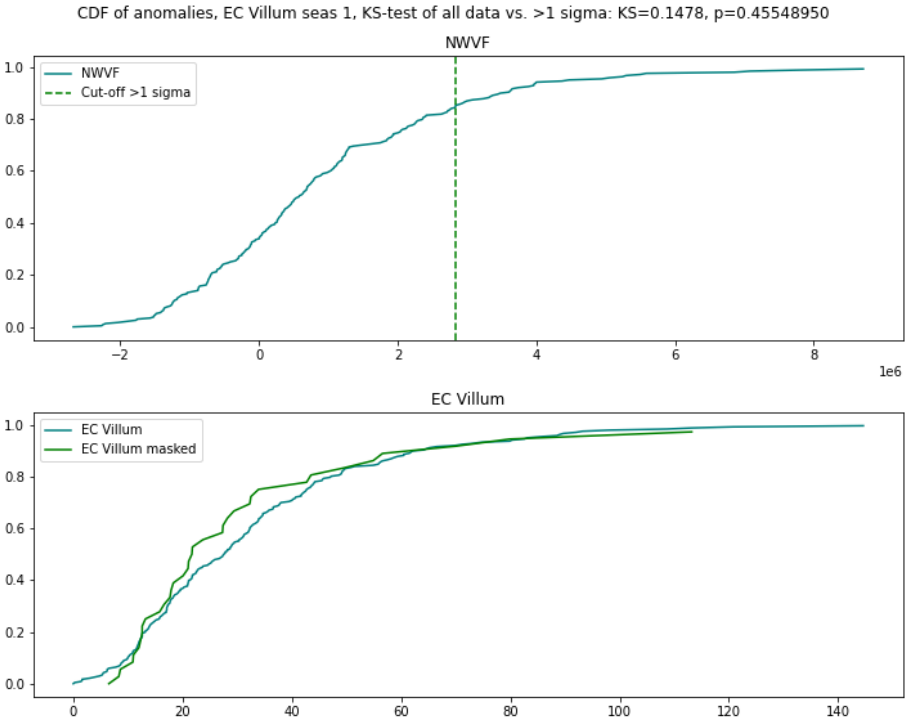

Figure 6 Cumulative distribution functions of NWVF and aerosols corresponding to the histograms in Figure 5. Upper panel shows the distribution of all NWVF values and the vertical line shows the +1 sigma cutoff used to mask the “events”. Lower panel shows in blue the distribution of all aerosol values and in green the distribution of the aerosols during the high-NWVF event days. The difference between these curves is the basis of the KS-test for significance of differences in the distributions (see text).

In Table 1, we show the results of performing the KS test on EC and SO_4 at Villum and Zeppelin stations for Seasons 1 and 2. Sample sizes are generally small and the KS distances are seen to be able to occur under the null hypothesis of the samples being drawn from the same distribution with quite high probability. The table shows p-values of 0.371-0.999 in all but the case of EC at Zeppelin in Season 1 where it is 0.09. Nevertheless, even this value does not allow us to claim significance of the difference at the 5 % level. Relative differences between the means of the two distributions are generally large, but the small sample sizes do not allow us to conclude any positive relationship between observed aerosols and high NWVF.

Table 1 Results of the KS test for EC and SO_4 at Villum and Zeppelin stations for Seasons 1 and 2. N_tot is the total number of observations during Seasons 1 and 2, respectively. N_pos is the number of observations during high NWVF conditions. KS is the vertical KS distance, p is the p value of the test (chance of KS distance occurring at random under the null hypothesis that distributions are the same) and "Rel diff" gives the difference between the mean value of the two distributions (to show the sign and magnitudes of the differences between them).

Species	Station	Season	N_tot	N_pos	KS	p	Rel diff
EC	Villum	1	236	36	0.1478	0.4554895	-10.3 %
		2	211	56	0.0537	0.9985116	-5.4 %
	Zeppelin	1	81	11	0.3816	0.0893988	-28.8 %
		2	85	20	0.1588	0.7496810	75.5 %
SO_4	Villum	1	311	48	0.1377	0.3713242	-10.6 %
		2	250	72	0.1073	0.4998239	-8.6 %

3.2 ERA5 NWVF vs MERRA reanalysis aerosols

The number of observed samples in the previous section was quite low, disallowing significant conclusions. Further, the station-based aerosol observations are of near-surface aerosols while aerosols throughout the troposphere are relevant for cloud formation and thereby climatic impact. Hence, we turn to aerosols from the MERRA-2 reanalysis which provides a full-column, spatially and temporally gap-free estimation of the aerosols.

We consider 25 years of data from the period 1997-01-01 to 2021-12-31 and compare aerosols from the MERRA-2 reanalysis with NWVF from the ERA5 reanalysis in the previous section. NWVF is still calculated across the red border in Figure 1, while aerosols are averaged over the band 70-75N latitude in the section 45W-45E, i.e., the 5-degree band just northward of the red border. Six different species are considered, namely black carbon (BC), organic carbon (OC), dust, SO_4, sea salt (SS) and $PM_{2.5}$. Further, we aggregate these into the total mass (summing all species) and a second aggregate we call "burden", calculated as, which is to mimic the total mass aggregate in the earth system model runs described in the next section. MERRA-2 assumes full neutralization of sulfate with ammonium, and since it only includes SO_4, but not NO_3 and NH_4, we use a constant of 1.375 to get the total secondary inorganic aerosol mass (i.e., sulfate + nitrate + ammonium = 1.375*sulfate) based on Buchard et al. (2016) and Song et al. (2018).

In the previous section, when the observations were considered, we did not use a daily climatology, since the length and gappiness of the records did not allow for this. Instead, we calculated monthly climatologies and further reduced the analysis to cover two separate seasons with separate means and separate anomalies. Here, the length of the record allows us to consider daily anomalies. For each species (and aggregate), we calculate anomalies (Figure 8) relative to a smooth climatology (Figure 7). This is done in the following steps:

- Calculate the 25-year average of all 1 Jan, 2 Jan, 3 Jan, …, 31 Dec. This results in a 365-day climatology, which is relatively noisy due to the 25-year length of the record.
- Perform a rolling 30-day average to produce a smooth climatology. This is shown for the NWVF and all species in Figure 7.

- In each of the 25 years, this climatology is subtracted from the raw signal (interpolating to 29 Feb in leap years) leading to the anomaly time series shown in Figure 8.

In the analysis of the observed aerosols, we used different standard deviations in the two seasons to determine what qualifies as a "high" NWVF event. Similarly, seasonal differences in variability are evident in the anomaly time series shown in Figure 8. Therefore, we calculated daily climatologies of the standard deviations to use as the threshold. This was done as follows:

- Since a standard deviation over only 25 instances of 1 Jan, 2 Jan, etc. is too noisy, we instead pooled anomalies from all January days and calculated a standard deviation for January, and repeated for all months Jan, ..., Dec. This is shown for NWVF as the black stepwise curve in Figure 9.
- Then we performed an interpolation between these monthly values to daily values, shown as the blue curve in Figure 9.
- The resulting 365-day climatology of standard deviations is then repeated each year and used to determine high-value events. This is illustrated, also for NWVF, in the upper panel of Figure 10 where the yellow lines show the seasonally varying 1 std threshold above which we define the anomaly to be a high NWVF event.

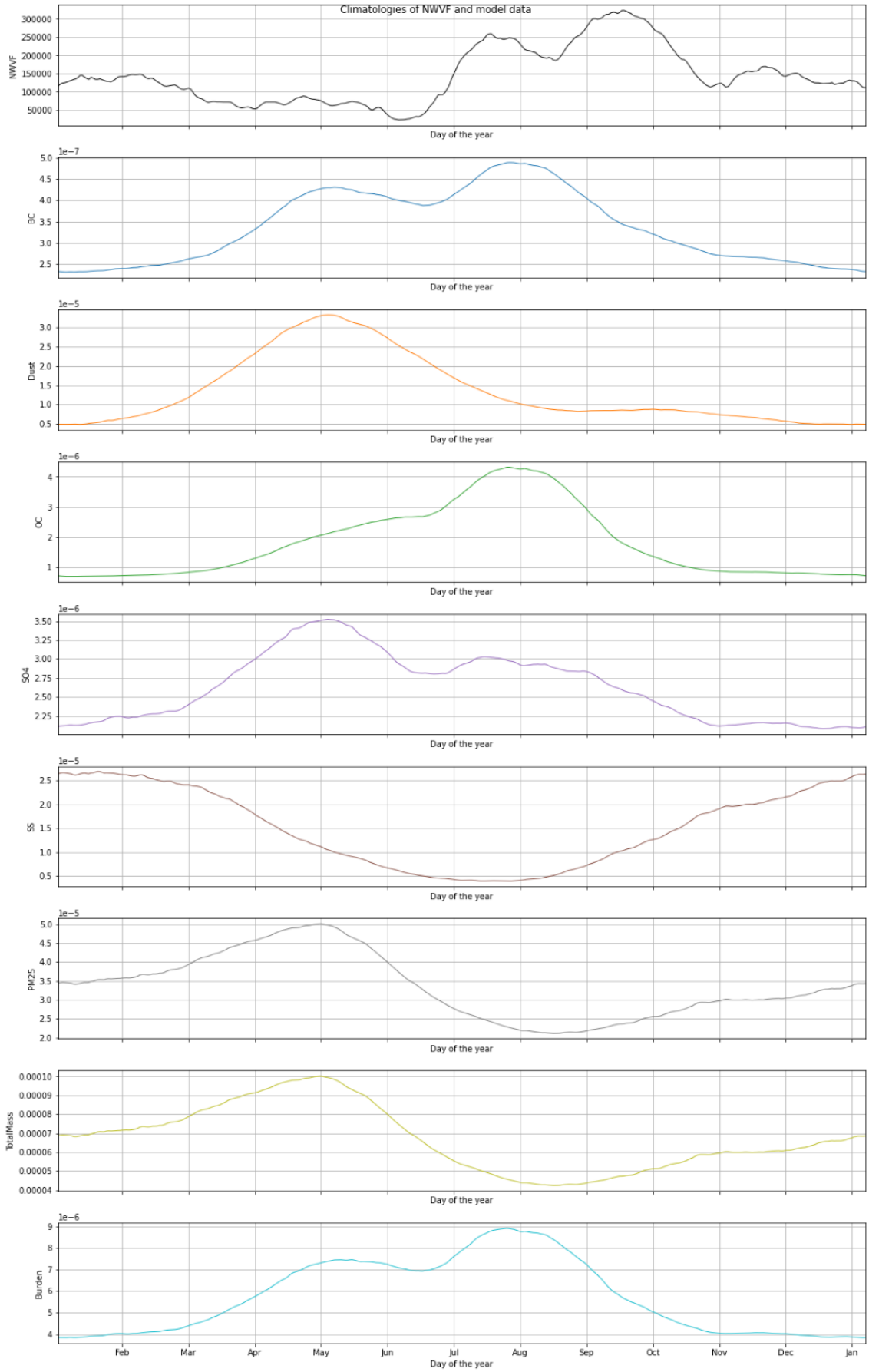

Figure 7 30-day rolling mean smoothed climatologies over the 25 years of 1997-2021 for ERA5 NWVF and the MERRA-2 reanalysis-based black carbon (BC), organic carbon (OC), dust, SO_4, sea salt (SS), $PM_{2.5}$, total mass (summing all species) and a second aggregate we call “burden”, calculated as BC+1.375* SO_4 +OC.

Figure 8 For NWVF and each of the MERRA-2 species and aggregates, the left hand panels show the anomaly time series calculated as the raw signals with the smoothed anomaly (Figure 7) subtracted. Right hand panels show the distributions.

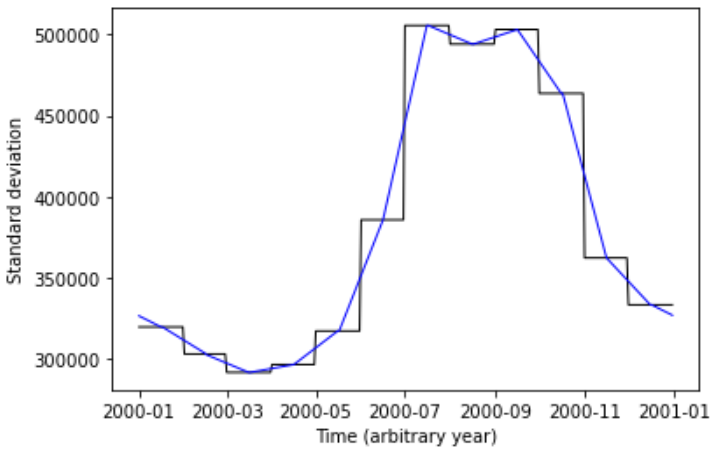

Figure 9 Illustration of calculation of seasonally varying standard deviation of NWVF. The black line shows the standard deviations calculated for each month by pooling all January, February, ..., December days, respectively. The blue line shows the interpolation to daily values used in the analyses.

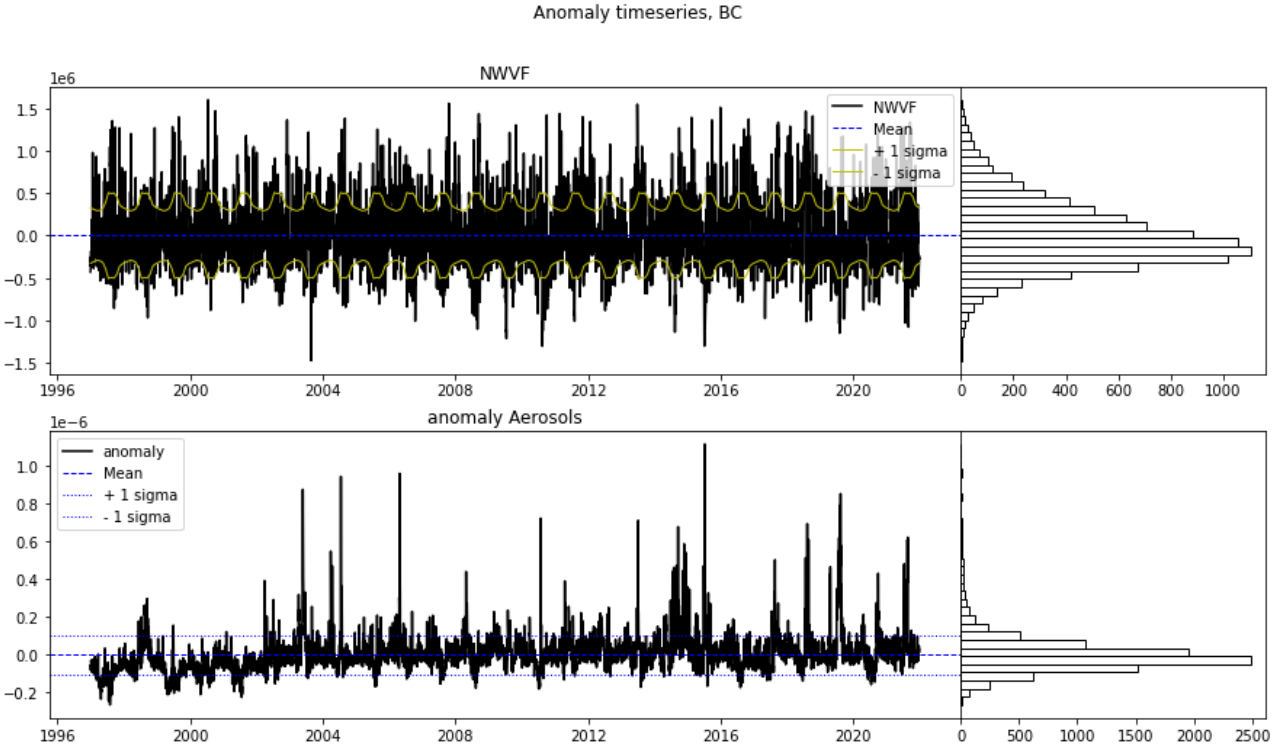

Figure 10 Anomalies of NWVF (upper) and BC (lower) as in Figure 8. Shown also for NWVF (yellow lines) is the seasonally varying climatology of standard deviations (from Figure 9) used as threshold to define high NWVF events. Note: It may seem that most days have values higher than the yellow curve, but this is only due to the thickness of the black curve. Of the 9131 days in the 25-year record, 1457 of them (about 16 %) are “high”. The right-hand plots show histograms of the two curves.

Figure 11 shows (similarly to Figure 5 for the observed record) the NWVF (upper panel) and BC (middle and lower panels) on all days (blue bars) and on high-NWVF days (green bars). Even when looking at the blue and green distributions of the BC on a logarithmic scale (lower panel), it is difficult to gauge whether the distributions are different. As previously, we perform a KS test and this is illustrated in Figure 12, where the lower panel shows the CDFs of the BC series on all days (blue) and masked to only the high-NWVF days (green). The statistics are shown in the top row of Table 2. Even with a KS distance of only 0.092, the large sample sizes make it virtually impossible (p= 0.0000000) to obtain if the samples were drawn from the same distribution. The green CDF lies to the right of the blue curve (relative difference of the

means is 4.8 %), and we conclude that during high-NWVF events, the BC concentration in the band-area is significantly increased by an average of 4.8 % compared to the all-days distribution. Figure 13 shows the same as Figure 12 but for the burden aggregate. This illustrates a case where the difference is positive (1.1 % increase relative to all-day distribution) but insignificant (p=0.086).

Table 2 gives the results of the KS test for all the species and the two aggregates. With the exception of OC and "burden" (BC+1.375* SO_4+OC), all differences are found to be significantly positive. This means that, as hypothesized, on days where NWVF is high, there is also an increased concentration of most species.

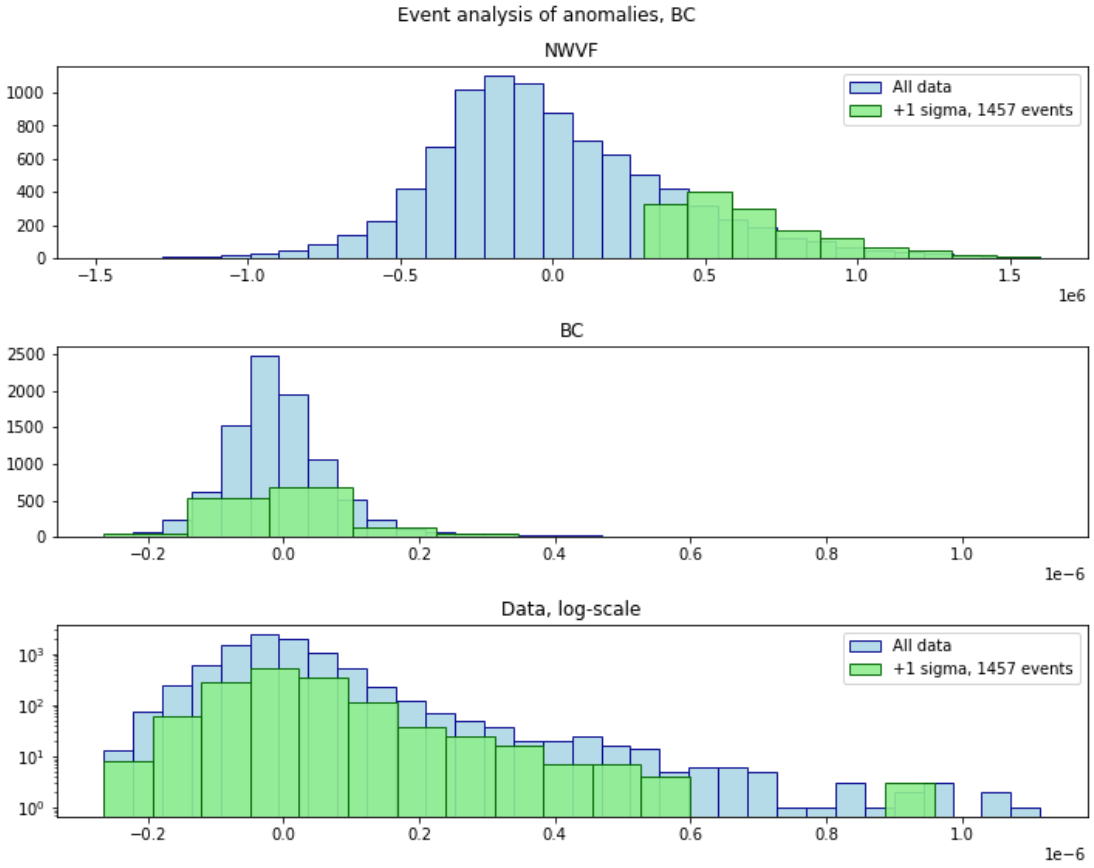

Figure 11 Upper: All NWVF "events" (blue), and +1 sigma events (green). Middle: All BC aerosol events (blue), the corresponding aerosol events that relate to the +1 sigma NWVF events (green). Lower: As for middle panel but with a logarithmic y-axis to allow easier comparison.

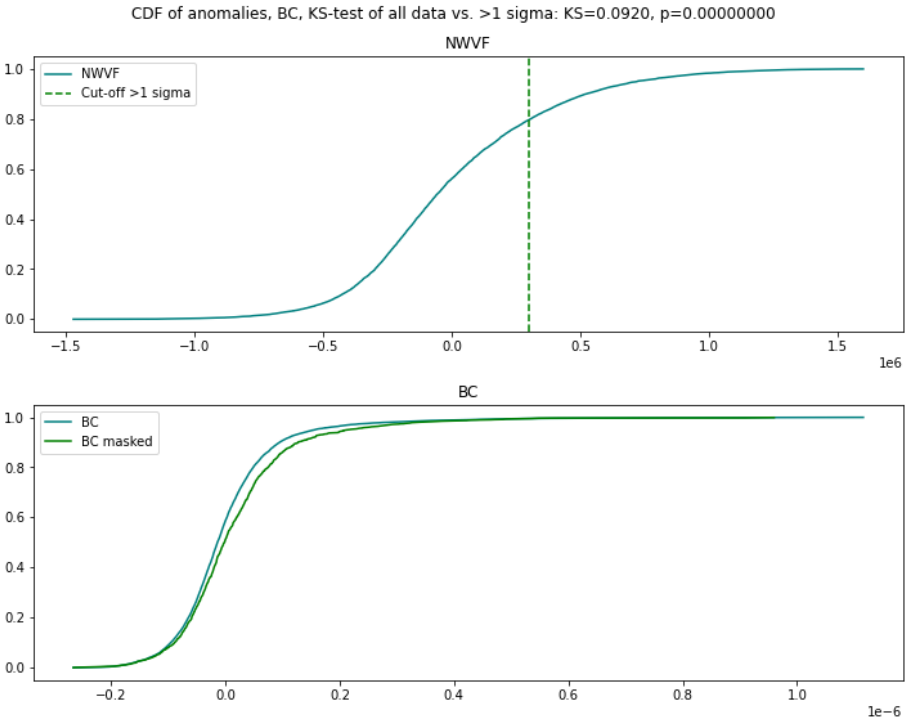

Figure 12 As Figure 6, but for the blue and green MERRA-2 BC distributions in the middle panel of Figure 11.

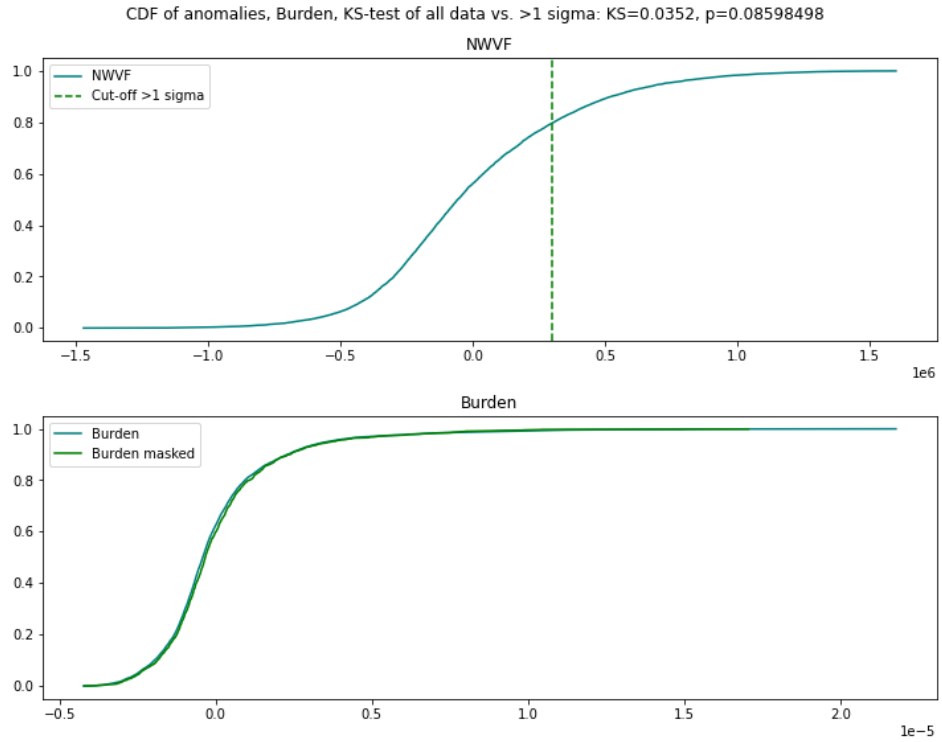

Figure 13 As Figure 12 but for the “burden” aggregate.

Table 2 Results of the KS test (like Table 1) for all species and aggregates in the MERRA-2 reanalysis. Burden is BC+1.375* SO_4+OC. N_tot is the total number of days and N_pos is the number of high-NWVF days. KS is the vertical KS distance, p is the p value of the test and "Rel diff" gives the difference between the mean values of the two distributions. Differences significant at the 5 % level are highlighted in bold italic.

Species	N_tot	N_pos	KS	P	Rel diff
BC	9131	1457	0.0920	***0.0000000***	***4.8%***
Dust	9131	1457	0.0386	***0.0463318***	***2.0%***
OC	9131	1457	0.0332	0.1219316	-1.2%
SO_4	9131	1457	0.0443	***0.0138333***	***1.9%***
SS	9131	1457	0.0689	***0.0000125***	***12.1%***
$PM_{2.5}$	9131	1457	0.0784	***0.0000003***	***6.4%***
TotalMass	9131	1457	0.0784	***0.0000003***	***6.4%***
Burden	9131	1457	0.0352	0.0859849	1.1%

3.3 GISS-E2 NWVF and aerosols

To investigate the interactions of aerosol and water vapor co-transports with clouds, we turn to the Earth System Model GISS-E2.1. This model is here run in two different configurations of the aerosol scheme:

- OMA, where the aerosols are interactively calculated from the sources, the atmospheric circulation and chemistry and the deposition processes.
- NINT, where the aerosols are non-interactive (hence, NINT) and are simply read in as monthly values from a file. The monthly values used here are taken as monthly averages from the OMA simulation. In the base case, referred here to as x1, the monthly values are used as is. Additionally, we make sets of the read-in aerosols where they have been multiplied by 5 and 10 before being read in. These simulations are referred to as x5 and x10, respectively.

First, we repeat the analysis from the previous section (on reanalysis-based NWVF and aerosols) but using output from the OMA simulation. NWVF was integrated over the same red border in Figure 1 and aerosols were averaged over the same 5-degree band.

Figure 14 shows the smoothed climatologies which may be compared to the reanalysis-based climatologies in Figure 7. The seasonal cycle pattern of the NWVF is very similar with low and decreasing values from January to mid-June, a double-peak in mid-July and mid-September of which the latter is strongest and finally a local minimum around early November. This gives us some confidence in the model's representation of the NWVF. However, turning to the aerosols, there are many differences in the patterns:

- BC has, correctly, a double peak, but the first one around early May is much too broad, and the second one is three months too late.
- OC has, correctly, a single peak with a shoulder to the left but the peak is too broad.
- SO_4 has, correctly, a double peak with the first one being stronger than the second, but they are both too late in the year – particularly the second one.

The NO_3 and NH_4 species were not represented in the MERRA-2 aerosol data. However, they both show a single peak in early June and these signals are so strong that the total OMA mass aggregate has this as its defining feature. In

MERRA-2 (Figure 7), neither BC, OC or SO_4 have this pattern, and the attempt to mimic OMA total mass with a linear combination of these as burden = BC+1.375* SO_4+OC (Figure 7 lower panel) is unlikely to succeed.

Subtracting the smoothed climatologies from the raw signals gave the anomalies shown in Figure 15. Comparing to the reanalysis-based anomalies in Figure 8, we see that, for example, the OMA OC signal is not as intermittent as that from MERRA-2 which has quiet periods interrupted by short, large excursions. On the other hand, the NO_3 and NH_4 signals which were not present in MERRA-2, both show this kind of behavior.

Given these anomalies, we calculated, as for the reanalysis, a climatological standard deviation which was used to determine the high-NWVF events. Table 3 shows the KS test results comparing the aerosols during the 1120 high-NWVF days to those during the full 7305 days (20 years). As opposed to the reanalysis case (Table 2), the BC, OC and SO_4 all show statistically significant negative relationships with NWVF (-4.3 %, -3.3 % and -5.6 %), meaning that during high-NWVF days, the aerosol loads are lower than normal. The difference for OC in MERRA-2 (Table 2) was also negative, but this was not significant.

Both NO_3 and NH_4 show quite intermittent anomalies (Figure 15), but for NO_3 this results in a strongly positive relationship (15.7 %) and for NH_4 it is very weakly negative (-0.4 %, but still significant).

All in all, this amounts to a significantly negative relationship for the total OMA burden (-4.0 %).

Table 3 Results of the KS test (like Table 2) for all species and the aggregate in the GISS-E2.1-OMA simulation.

Species	N_tot	N_pos	KS	P	Rel diff
BC	7305	1120	0.1136	0.0000000	-4.3 %
OC	7305	1120	0.0890	0.0000003	-3.3 %
SO_4	7305	1120	0.2240	0.0000000	-5.6 %
NO_3	7305	1120	0.0610	0.0013781	15.7 %
NH_4	7305	1120	0.0699	0.0001417	-0.4 %
BC+OC+ SO_4+ NO_3+ NH_4	7305	1120	0.1746	0.0000000	-4.0 %

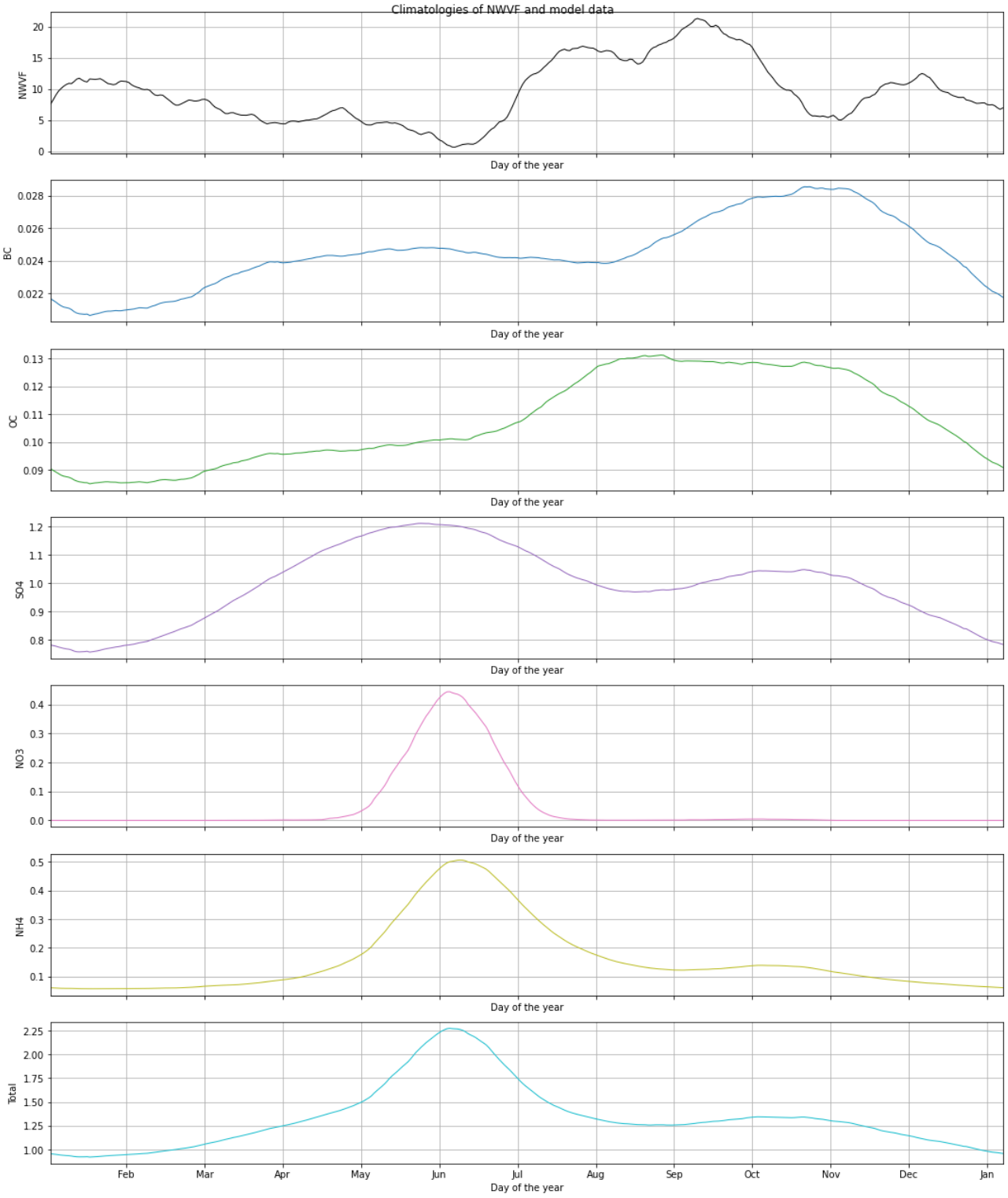

Figure 14 30-day rolling mean smoothed climatologies over the 20 years of 1995-2014 for GISS-E2.1-OMA based NWVF and aerosols black carbon (BC), organic carbon (OC), SO_4, NO_3 and NH_4 and their total mass (the latter was approximated in the MERRA analysis as burden=BC+1.375* SO_4+OC.

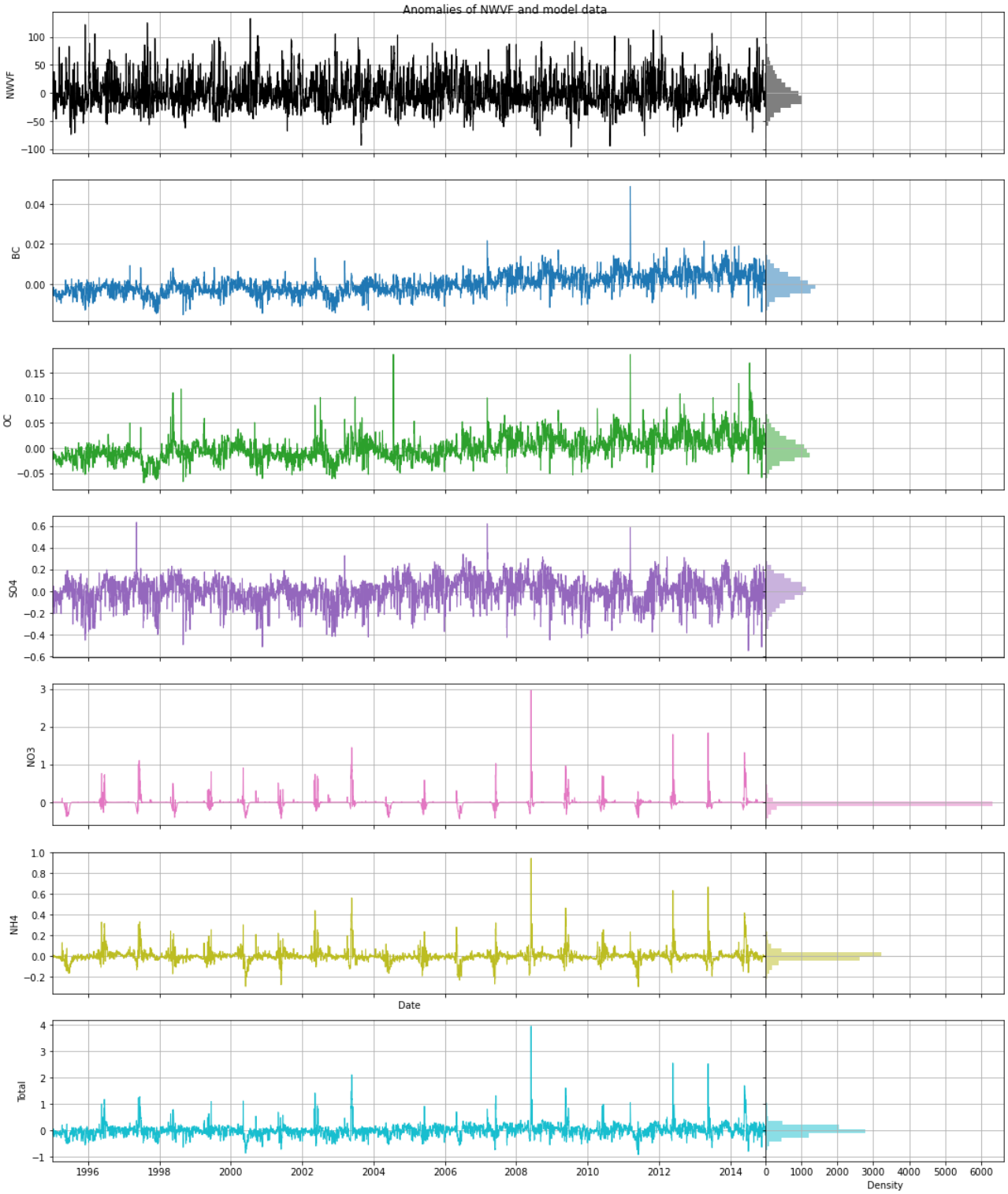

Figure 15 Anomalies for the GISS-E2.1-OMA simulation derived like those in Figure 8 for the reanalysis-based species.

3.4 GISS-E2.1 NWVF and clouds

Finally, we turn to the relationship between NWVF, aerosols and clouds. For cloud amount, we use the variables liquid (lwp) and ice (iwp) water path averaged over the same 5 degree band as above. Table 4 shows the results of the KS test looking at lwp and iwp on high-NWVF days compared to all days. Unsurprisingly, on days where the NWVF is high, there is a strongly increased cloudiness in the band.

Table 4 Results of the KS test comparing liquid (lwp) and ice (iwp) water path distribution during high-NWVF conditions to the all-days distribution in the GISS-E2.1-OMA simulation.

Cloud	N_tot	N_pos	KS	P	Rel diff
lwp	7305	1120	0.3703	0.0000000	42.0 %
iwp	7305	1120	0.2079	0.0000000	38.8 %

The next question is whether increasing the aerosol amounts will lead to further increases in cloudiness under high-NWVF conditions. To answer this question, we turn to the NINT simulations where we have control over the aerosol amounts and can synthetically boost them to very high levels. Table 5 shows the results of this analysis. The total number of days in the analysis is the same (7305, 20 years) but the weather evolution is slightly different leading to almost, but not exactly, the same number of high-NWVF days in OMA, NINT-x1, NINT-x5 and NINT-x10. The increases in clouds are very similar across all three NINT experiments, and they even closely resemble those in the OMA simulation (Table 4) - not just in the relative difference, but even also in the KS distance.

Apparently, in this model, increasing the aerosol amounts does not reinforce the increase in lwp and iwp during high-NWVF events. A final test shows this clearly in Table 6, where the high-NWVF cloud distributions are compared between x5 and x1 and between x10 and x1. In both cases, the relative difference is very close to zero and the p-values are above 99 %. There is clearly no significant difference between the high-NWVF cloud distributions in the three different aerosol backgrounds.

Table 5 Results of the KS test comparing liquid (lwp) and ice (iwp) water path distribution during high-NWVF conditions to the all-days distribution in the GISS-E2.1-NINT x1, x5 and x10 simulations.

Aero multi	Cloud	N_tot	N_pos	KS	P	Rel diff
x1	lwp	7305	1117	0.3633	0.0000000	42.3 %
	iwp	7305	1117	0.2081	0.0000000	38.5 %
x5	lwp	7305	1118	0.3591	0.0000000	42.2 %
	iwp	7305	1118	0.2076	0.0000000	39.3 %
x10	lwp	7305	1116	0.3575	0.0000000	42.1 %
	iwp	7305	1116	0.2137	0.0000000	39.5 %

Table 6 Results of the KS test comparing cloud amounts on high-NWVF days in x5 vs x1 and x10 vs x1, respectively. That is, asking whether the cloud amount is higher when there is high NWVF in x5 (or x10) than when there is high NWVF in x1.

Aero multi	Cloud	KS	P	Rel diff
x5 vs x1	lwp	0.0116	0.99999928	0.0 %
	iwp	0.0179	0.99401333	0.8 %
x10 vs x1	lwp	0.0146	0.99962608	-0.1 %
	iwp	0.0141	0.99977614	0.8 %

4 Discussion and conclusions

In the MERRA-2 reanalysis aerosol data, the OC species shows (Figure 8) a somewhat different pattern of anomalies from the other species with small variations interrupted by few very large positive excursions. The large excursions tend not to occur during high NWVF conditions and perhaps these fluctuations during non-high NWVF days tend to counter the effects of heightened OC in the small-variance part of the series during high-NWVF days. Further, the addition of OC to the burden statistic means that this carries some of the same characteristics with a few very high excursions during non-high NWVF days. This is not enough to make the relative difference negative (it is +1.1 %) but enough to render the difference insignificant (Table 2).

Further, the strong increase in MERRA-2 reanalysis sea salt (SS) during high NWVF (Table 2) may be due to increased local mobilization associated with the wind fetch during the event. This is not present in the other, long-range transported species.

In the GISS-E2.1-OMA simulation, apparently both the climatology (Figure 14) and the variability (Figure 15) of the simulated aerosols are somewhat different from those in the reanalysis (Figure 7 and Figure 8) and we may not be able to expect their co-variability with NWVF to match the reanalysis. Looking at the anomaly time series (Figure 15), there appears to be an upward trend in some of the data. This is likely to be associated with long-term climate change which may be realistic, but this may impact the robustness of our statistical tests which assume temporal stationarity in the underlying distributions. Therefore, we repeated the analysis after first detrending the signal (to focus on the short-term variability). However, this did not change the results in any qualitative way.

Further, one may wonder if the lack of a positive relationship in the model results is associated with the timescale it takes for the increased northward transports to manifest as heightened aerosol loads in the northward band. To test this, we repeated the analysis using 3 day (and 5 day) running means on all the series. Again, this did not qualitatively change the results.

In conclusion,

- The station-based observations are too few to allow for statistically significant conclusions regarding the co-occurrence of high NWVF with increased aerosol amount (Table 1).
- The reanalysis show significantly increased aerosols during high NWVF for all species except for OC which has a particularly intermittent behavior which appears distinct from the NWVF (Table 2).
- In the Earth System Model, GISS-E2.1-OMA, with interactively calculated aerosols, the climatology of the NWVF resembles that from the reanalysis well. The different aerosol species, however, show some important differences from their reanalysis counterparts. Despite having single-, double- or shoulder-peak patterns in common, their timings throughout the year appear off. Moreover, for OC the intermittent pattern of the anomaly time series is absent. Instead, this is seen in the NO_3 and NH_4 series.
- Not only are the climatologies and characteristics of the anomaly time series different from the reanalysis, the positive relationship between

aerosols and high NWVF from the reanalysis is rather a significantly negative relationship in GISS-E2.1-OMA.

- During high NWVF, both model versions (OMA and NINT) unsurprisingly display increased cloudiness. However, increasing the aerosol amounts appears not to influence how large the increase in cloudiness is during high-NWVF conditions.
- If the latter is generally true, this would mean that, even if, as the reanalysis may suggest, there is increased aerosol amount during high NWVF, this would not lead to increased cloudiness and would not by that pathway impact Arctic climate.

More work remains to investigate the differences between the statistical characteristics of the modeled and reanalysis climatology and variability of the common aerosol species. Only when these differences are understood can we truly hope to understand the differences between the reanalysis and modeled co-transports of moisture and aerosols. Further, several processes related to aerosol-cloud interactions are still under development. Therefore, the above conclusion is unlikely to be the final word on the matter.

References

AMAP, 2017: Snow, Water, Ice and Permafrost in the Arctic (SWIPA) 2017. Arctic Monitoring and Assessment Programme (AMAP), Oslo, Norway. xiv + 269 pp. 269 pp.

AMAP, 2021: Arctic Climate Change Update 2021: Key Trends and Impacts. Summary for Policy-makers. Arctic Monitoring and Assessment Programme (AMAP), Tromsø, Norway. 16 pp.

Baggett, C. & S. Lee, 2017: An Identification of the Mechanisms that Lead to Arctic Warming During Planetary-Scale and Synoptic-Scale Wave Life Cycles. J. Atmospheric Sci., 74, 1859–1877, https://doi.org/10.1175/JAS-D-16-0156.1.

Bauer, S. E. & Coauthors, 2020: Historical (1850–2014) Aerosol Evolution and Role on Climate Forcing Using the GISS ModelE2.1 Contribution to CMIP6. J. Adv. Model. Earth Syst., 12, e2019MS001978, https://doi.org/10.1029/2019MS001978.

Buchard, V. & Coauthors, 2016: Evaluation of the surface PM2.5 in Version 1 of the NASA MERRA Aerosol Reanalysis over the United States. Atmos. Environ., 125, 100–111, https://doi.org/10.1016/j.atmosenv.2015.11.004.

C3S, 2017: Copernicus Climate Change Service, ERA5: Fifth generation of ECMWF atmospheric reanalyses of the global climate . Copernicus Climate Change Service Climate Data Store (CDS) https://cds.climate.copernicus.eu/cdsapp#!/home.

Dekoutsidis, G., M. Wirth & S. Groß, 2024: The effects of warm-air intrusions in the high Arctic on cirrus clouds. Atmospheric Chem. Phys., 24, 5971–5987, https://doi.org/10.5194/acp-24-5971-2024.

Francis, J.A. & S.J. Vavrus, 2012: Evidence linking Arctic amplification to extreme weather in mid-latitudes. Geophys. Res. Lett., 39, https://doi.org/10.1029/2012GL051000.

Graversen, R.G. & M. Burtu, 2016: Arctic amplification enhanced by latent energy transport of atmospheric planetary waves. Q. J. R. Meteorol. Soc., 142, 2046–2054, https://doi.org/10.1002/qj.2802.

Hansen, J. & Coauthors, 2005: Efficacy of climate forcings. J. Geophys. Res. Atmospheres, 110, https://doi.org/10.1029/2005JD005776.

Im, U. & Coauthors, 2021: Present and future aerosol impacts on Arctic climate change in the GISS-E2.1 Earth system model. Atmos Chem Phys, 21, 10413–10438, https://doi.org/10.5194/acp-21-10413-2021.

Kelley, M. & Coauthors, 2020: GISS-E2.1: Configurations and Climatology. J. Adv. Model. Earth Syst., 12, e2019MS002025, https://doi.org/10.1029/2019MS002025.

Langen, P.L. & V.A. Alexeev, 2007: Polar amplification as a preferred response in an idealized aquaplanet GCM. Clim. Dyn., 29, 305–317, https://doi.org/10.1007/s00382-006-0221-x.

Lapere, R. & Coauthors, 2024: Polar Aerosol Atmospheric Rivers: Detection, Characteristics, and Potential Applications. J. Geophys. Res. Atmospheres, 129, e2023JD039606, https://doi.org/10.1029/2023JD039606.

Lenssen, N.J.L., G.A. Schmidt, J.E. Hansen, M.J. Menne, A. Persin, R. Ruedy, & D. Zyss, 2019: Improvements in the GISTEMP Uncertainty Model. J. Geophys. Res. Atmospheres, 124, 6307–6326, https://doi.org/10.1029/2018JD029522.

Menon, S. & L. Rotstayn, 2006: The radiative influence of aerosol effects on liquid-phase cumulus and stratiform clouds based on sensitivity studies with two climate models. Clim. Dyn., 27, 345–356, https://doi.org/10.1007/s00382-006-0139-3.

Miller, R.L., G.A. Schmidt & D.T. Shindell, 2006: Forced annular variations in the 20th century Intergovernmental Panel on Climate Change Fourth Assessment Report models. J. Geophys. Res. Atmospheres, 111, https://doi.org/10.1029/2005JD006323.

Rantanen, M., A. Yu. Karpechko, A. Lipponen, K. Nordling, O. Hyvärinen, K. Ruosteenoja, T. Vihma & A. Laaksonen, 2022: The Arctic has warmed nearly four times faster than the globe since 1979. Commun. Earth Environ., 3, 168, https://doi.org/10.1038/s43247-022-00498-3.

Rayner, N.A., D.E. Parker, E.B. Horton, C.K. Folland, L.V. Alexander, D.P. Rowell, E.C. Kent & A. Kaplan, 2003: Global analyses of sea surface temperature, sea ice, and night marine air temperature since the late nineteenth century. J. Geophys. Res. Atmospheres, 108, https://doi.org/10.1029/2002JD002670.

Reynolds, R.W., N.A. Rayner, T.M. Smith, D.C. Stokes & W. Wang, 2002: An Improved In Situ and Satellite SST Analysis for Climate. J. Clim., 15, 1609–1625, https://doi.org/10.1175/1520-0442(2002)015<1609:AIISAS>2.0.CO;2.

Song, Z. & Coauthors, 2018: Diurnal and seasonal variability of PM2.5 and AOD in North China plain: Comparison of MERRA-2 products and ground measurements. Atmos. Environ., 191, 70–78, https://doi.org/10.1016/j.atmosenv.2018.08.012.

Taylor, P.C. & Coauthors, 2022: Process Drivers, Inter-Model Spread, and the Path Forward: A Review of Amplified Arctic Warming. Front. Earth Sci., 9.

Woods, C. & R. Caballero, 2016: The Role of Moist Intrusions in Winter Arctic Warming and Sea Ice Decline. J. Clim., 29, 4473–4485, https://doi.org/10.1175/JCLI-D-15-0773.1.

Yoshimori, M.,A. Abe-Ouchi & A. Laîné, 2017: The role of atmospheric heat transport and regional feedbacks in the Arctic warming at equilibrium. Clim. Dyn., 49, 3457–3472, https://doi.org/10.1007/s00382-017-3523-2.

COINCIDING TRANSPORTS OF WATER VAPOR AND AEROSOLS TO THE ARCTIC

– in observations, reanalysis data and earth system model simulations

This study investigates statistics of moisture and aerosol transports to the Arctic. In an atmospheric reanalysis product, we find a significant positive relationship, with increased column-total aerosol amounts during high northward water vapor transport events, for most of the species considered. In an Earth System Model, we find that the positive relationship between aerosols and high northward water vapor transport from the reanalysis is rather a significantly negative relationship and, further, that increasing the aerosol amounts appears not to influence how large that increase in cloudiness is during high water vapor transport events. However, there are still many unanswered questions and much work to do to fully understand the discrepancy between the model and the reanalysis, and several processes related to aerosol-cloud interactions are still under development.

ISBN: 978-87-7156-920-9
ISSN: 2244-9981